

Chemisorption of sulfur on nickel: A study of cluster convergence in the linear combination of Gaussian-type orbitals local density functional approach

L. Ackermann and N. Rösch

Citation: *The Journal of Chemical Physics* **100**, 6578 (1994); doi: 10.1063/1.467067

View online: <http://dx.doi.org/10.1063/1.467067>

View Table of Contents: <http://scitation.aip.org/content/aip/journal/jcp/100/9?ver=pdfcov>

Published by the **AIP Publishing**

Articles you may be interested in

[A two-component variant of the Douglas–Kroll relativistic linear combination of Gaussian-type orbitals density-functional method: Spin–orbit effects in atoms and diatomics](#)

J. Chem. Phys. **115**, 4411 (2001); 10.1063/1.1390509

[Structural features of the NO/Ru\(001\) adsorption complexes: A linear combination of Gaussian-type orbitals local density functional model cluster analysis of high-resolution electron energy loss spectroscopy data](#)

J. Chem. Phys. **100**, 2310 (1994); 10.1063/1.466529

[Comment on: Relativistic linear combination of Gaussian-type orbitals density functional method based on a two-component formalism with external field projectors](#)

J. Chem. Phys. **96**, 6320 (1992); 10.1063/1.462625

[Relativistic linear combination of Gaussian-type orbitals density functional method based on a two-component formalism with external field projectors](#)

J. Chem. Phys. **92**, 1153 (1990); 10.1063/1.458177

[Analytical gradient of the linear combination of Gaussian-type orbitals—local spin density energy](#)

J. Chem. Phys. **90**, 6371 (1989); 10.1063/1.456354



Chemisorption of sulfur on nickel: A study of cluster convergence in the linear combination of Gaussian-type orbitals local density functional approach

L. Ackermann and N. Rösch

Lehrstuhl für Theoretische Chemie, Technische Universität München, 85747 Garching, Germany

(Received 8 October 1993; accepted 11 January 1994)

Chemisorption of sulfur at the (100), (110), and (111) surface of nickel has been studied, using the linear combination of Gaussian-type orbitals local density functional (LCGTO-LDF) method. Employing various cluster models consisting of 11 to 29 substrate atoms, adsorption at the experimentally known sites has been considered. Besides the equilibrium distance and the force constant of the vertical adsorbate motion, the dynamical dipole moment was evaluated and it turned out to provide a sensitive probe of cluster convergence. The influence of atoms from the third substrate layer on the various observables is found to be considerable in some cases. With increasing cluster size, bond lengths are stabilized to 0.02 Å, frequencies to 20 cm⁻¹, and dipole moments to 0.1 D. The converged results agree very well with experiment. Adsorption induced population changes are restricted to only four to six neighboring substrate atoms of the modifier atom. However, energy resolved charge density differences reveal a possible mechanism for the transmission of the long-range electronic effects caused by the adatom.

I. INTRODUCTION

Sulfur chemisorption on nickel has been studied extensively, both theoretically and experimentally.¹⁻²⁸ Various scattering and diffraction techniques have furnished information for the three low index surfaces. Bond distances, vibrational frequencies, and binding energies have been determined in many cases.¹⁻²² Therefore, the chemisorption system Ni/S, allowing a detailed comparison, may be used to test the accuracy and predictive capability of a theoretical description. Also, the poisoning influence of sulfur (and other electronegative atoms like C or P) on catalytically active substrates and the electronic origin of this effect is studied with growing intensity.^{1,29}

Several theoretical investigations of the system Ni/S have been carried out, employing a variety of methodologies. Some focus on the interaction of sulfur and nickel per se;²³⁻²⁵ other studies include the coadsorption of CO molecules, analyzing the range and mechanism of the effect exerted on the chemisorptive bond by the modifier atom.²⁶⁻²⁸ The objective of the present work is twofold: (i) limitations of the cluster model description are analyzed for the example of sulfur chemisorption on nickel and (ii) the results obtained for this system are discussed and compared to experimental data.

Cluster models provide a popular and successful approach to the theoretical study of chemisorption systems.³⁰ Abandoning the translational symmetry exploited in slab models and confining the substrate to a few atoms in the vicinity of the adsorption site, this description operates within the picture of a rather localized chemisorption interaction. The quality of a calculation based on this technique depends severely on the size of the model cluster. This very general observation must be supplemented with more specific statements to be helpful in the actual construction of suitable cluster models. The most basic demand, namely that the environment of each atom in the model should represent

reality as close as possible, clearly calls for large clusters. This claim naturally conflicts with computational economy, which leads to the question: How big a cluster is necessary to reduce the inherent error of the model description below a given threshold? Of course, not only the size of a model, but also its geometric and electronic structure^{31,32} determine its ability to approximate a real surface. It is worthwhile to explore how successful different clusters of a given size are in this respect.

It is common to analyze a series of cluster models for a given adsorption site. They are intended to represent the same physical situation, but differ in size and shape. Therefore it is important to monitor the convergence behavior by taking into account not only a single quantity, but as many as possible. Bond distances, vibrational frequencies, and binding energies are commonly used to judge the cluster size dependence of the model (e.g., Ref. 33). These quantities are expected to reflect the general trend of convergence; they represent the backbone of the analysis presented in Sec. III A. Furthermore, the induced dipole moment as a function of the adsorbate-substrate distance is used in this analysis of cluster models. It turns out to yield a very sensitive probe for differences between various models of increasing size.

Other recent cluster studies have focused on the convergence of the binding energy.^{31,32,34} The concept of "bond preparation" has been developed and successfully applied to various chemisorption problems. In this approach the calculated binding energy within a series of cluster models is stabilized by using a suitable excited state of the bare cluster as a reference, if required by the underlying bonding mechanism. It has been demonstrated that the oscillatory behavior of the binding energy in a cluster series can be reduced significantly by this technique.³² For technical reasons (see below) it is not possible, however, to apply this technique in the approach used for this study. Without bond preparation the binding energy must be regarded as a less reliable indicator

TABLE I. Properties of the low index surfaces of an fcc crystal. The spacing between the crystal layers (neglecting surface relaxation) is given in units of the metal-metal distance. *S* is the highest-coordinated adsorption site, A1 and B1 are the groups of symmetry equivalent atoms closest to the adsorbate in the first and second layer, respectively (see Fig. 1). The coordination refers to the number of adjacent substrate atoms.

Surface	Site symmetry	Layer spacing	Nearest-neighbor coordination		
			<i>S</i>	A1	B1
110	C_{2v}	0.50	5	7	11
100	C_{4v}	0.71	4	8	12
111	C_{3v}	0.82	3	9	12

of cluster convergence and thus will be used in the following discussion only sparingly.

When building clusters and enlarging them in a systematic way, one may be guided by various concepts, most of which have a somewhat intuitive character. An obvious approach is to think in terms of crystal layers. Moving along the surface normal (chosen to be the *z* axis) towards the bulk, the importance of substrate atoms in the description of chemisorption decreases. Experimental and theoretical evidence from a variety of studies on large metal clusters indicates that atoms with three or more shells of neighbors acquire essentially bulk-like properties.^{35,36} The idea of convergence by crystal layers should be applied cautiously, however, when surfaces of different structure are considered. For example, going from the rather open (110) to the compact (111) surface of an fcc crystal, the interlayer distance increases substantially (Table I). This quantity is proportional to the atom density within a crystal layer, assuming the same spatial packing in each case. Naturally, this leads to a somewhat different relation between the number of layers and the convergence behavior for the various surfaces.

Another very appealing criterion in the construction of clusters is the distance of a substrate atom from the adsorbate. In the limit, this procedure leads to cluster models of roughly semispherical shape; however, it neglects the differences of screening effects for the surface and the bulk atoms of the substrate, especially for clusters of limited size.

In the present study we adopt a scheme that lies somewhere in between. It is based on the concept of neighborhood relationships. The adatom interacts most strongly with the metal atoms closest to it. They, in turn, should have a coordination as close as possible to that in the real surface (Table I). Many of the resulting clusters do conform to the concepts mentioned above, others do not. In some cases alternative models have been tested, allowing a comparison of the relative importance of different groups of substrate atoms for the model description.

A prerequisite for an extensive analysis of cluster convergence of various properties is a method that allows the treatment of large clusters. In wave function based *ab initio* calculations this can only be achieved by using pseudopotentials for the description of core electrons.^{23,32} This technique has recently been employed in a cluster model study of sulfur on nickel that uses a Ni_{25} cluster.²³ On the other hand, the explicit description of core electrons allows an adequate rep-

resentation of subvalence orbitals. To treat systems of the required size in an all-electron approach, however, a powerful alternative to wave function based *ab initio* methods is needed. Here the linear combination of Gaussian-type orbitals local density functional (LCGTO-LDF) method³⁷ has its merits, allowing high standard electronic structure calculations involving more than 1000 electrons.³⁸

II. COMPUTATIONAL DETAILS

A. Electronic structure method

The electronic density of the ground state of a system, ρ , the central quantity of the density functional theory can be calculated self-consistently from the Kohn-Sham equations.³⁹ In the LCGTO-LDF implementation³⁷ this is performed by employing a Gaussian functional basis. Two additional basis sets, utilized for fitting ρ and the exchange-correlation potential v_{ex} are derived from the molecular orbital (MO) basis.^{40,41} For nickel, a (15s/11p/6d) (Ref 42) and for sulfur a (12s/9p/2d) MO basis⁴³ was used. Full contractions of the MO basis sets were obtained from the solution of atomic LDF calculations, resulting in (6s/5p/3d) and (5s/4p/2d) basis sets for Ni and S, respectively.

Prior to the study of convergence, the smallest cluster of each series was treated using different local approximations to the exchange-correlation potential v_{ex} . Comparing the standard $X\alpha$ potential ($\alpha=0.7$) and the Vosko-Wilk-Nusair parametrization,⁴⁴ only small differences were found in all calculated quantities. In the latter case, equilibrium bond lengths were 0.01–0.03 Å shorter, frequencies 10–20 cm⁻¹, and binding energies 0.5–0.75 eV higher than in the first case. From these results, the influence of the choice of the exchange-correlation approximation, although not negligible, was considered to be of minor importance in the present context, since the cluster effects studied do not explicitly depend on this detail of calculation. For the same reason it did not seem necessary to go beyond the local density approximation. For the remainder of this study the $X\alpha$ potential is used. Working with a spin-polarized scheme³⁷ allows the analysis of the influence of the adsorbate on the magnetic properties of the substrate.

Nickel clusters of the size used in chemisorption studies have a rather dense, though discrete, spectrum around the Fermi energy. Motivated by the situation at a real surface, a formal Gaussian level broadening (0.3 eV) was used, which permits the self-consistent determination of a cluster Fermi energy from the resulting continuous density of states (DOS).⁴² This procedure implies fractional occupation numbers (FON) which, in a formal sense, could also have been introduced by averaging over the manifold of states that is virtually degenerate to the ground state.^{41,42} In any case, the formal level broadening yields a reasonably stable numerical procedure which allows a consistent treatment of fairly large metal clusters.

B. Cluster models for chemisorption

For all models, the geometrical variation is confined to the motion of the adsorbate normal to the surface. The corresponding coordinate will be denoted by d_{\perp} . A series of five

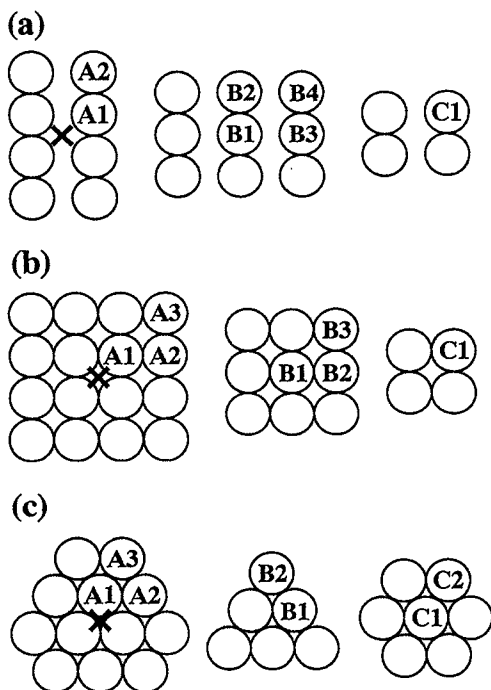


FIG. 1. Atoms of the three topmost crystal layers (labeled A, B, and C) are used to construct cluster models of the surfaces Ni(110) (a), Ni(100) (b), and the fcc site on Ni(111) (c). In the clusters modeling the hcp site of Ni(111), the atoms of the second and third layer of the fcc cluster models are interchanged. The adsorbate position is marked (x) in the first layer.

or six points was used to determine the equilibrium position of sulfur and the associated frequency ω_{\perp} . The latter is calculated by numerically integrating the vibrational Schrödinger equation for the fitted potential. Its value was found to deviate from a harmonic fit by 5 cm^{-1} at most.

Additional points (up to $d_{\perp} \approx 2.2 \text{ Å}$) have been included to explore the distance dependence of the dipole moment $\mu(d_{\perp})$ in the region where an essentially linear variation was encountered (see Sec. III B). Due to symmetry, the dipole moment has only one relevant component (in the z direction). Its change in the course of chemisorption (the induced dipole moment) is defined as the difference $\Delta\mu = \mu(\text{Ni}_n\text{S}) - \mu(\text{Ni}_n)$.

The clusters are chosen to model the chemisorption of sulfur on Ni(110), Ni(100), and Ni(111). From experiment⁴ it is known that sulfur is adsorbed with maximum coordination (Table I). On the (111) surface cluster models for both the fcc and the hcp site are studied, the former being found experimentally.^{4,9,11} In Fig. 1 the structures of the largest models are sketched. Groups of atoms that are equivalent by symmetry are labeled by letters (A–C) indicating the crystal layer and by an additional number. The clusters Ni_n chosen for the study are presented in Table II. A detailed composition of clusters specifying the number of atoms per crystal layer is given in parentheses whenever necessary for discrimination. Nearest-neighbor nickel–nickel distances are kept fixed to the bulk value, 2.49 Å .

On the (110) surface the adsorption site of fivefold co-

TABLE II. Structure and classification of cluster models. The composition of each crystal layer is summarized in parentheses. The detailed information refers to the numbering introduced in Fig. 1. The last two columns indicate how many nickel atoms adjacent to A1 (B1) are part of the cluster.

Surface	Ni_nS	Unique atoms ^a	Coordination of A1	Coordination of B1
110	11 (8,3)		4	6
	13 (8,5)	B3	5	6
	15 (8,3,4)	C1	5	10
	17 (8,5,4)	B3, C1	6	10
100	21 (8,9,4)	B3, B4, C1	7	10
	17 (12,5)		7	8
	21 (16,5)	A3	7	8
	21 (12,9)	B3	8	8
	21 (12,5,4)	C1	7	12
111 (fcc)	29 (16,9,4)	A3, B3, C1	8	12
	12 (6,6)		7	7
	18 (6,6,6)	C2	7	9
	19 (6,6,7)	C1, C2	7	10
111 (hcp)	18 (12,6)	A3	9	7
	25 (12,6,7)	A3, C1, C2	9	10
	13 (6,7)		7	9
	16 (6,7,3)	C1	7	12
	19 (6,7,6)	C1, C2	7	12
	19 (12,7)	A3	9	9
	22 (12,7,3)	A3, C1	9	12
	25 (12,7,6)	A3, C1, C2	9	12

^aAll clusters contain atoms A1, A2, B1, and B2.

ordination is represented by the atoms A1 and B1. This minimal (4,1) cluster is extended in the $[1\bar{1}0]$ direction (parallel to the ridges) by A2 and B2, respectively, giving the smallest cluster of the series, $\text{Ni}_{11}(8,3)$. Within each layer the atoms closest to the adsorption site are saturated with their nearest neighbors. Starting from this model, larger ones are obtained by adding second and third layer atoms. The group of equivalent atoms in the third layer, C1, is part of the three largest clusters, Ni_{15} , Ni_{17} , and Ni_{21} , but not of the smaller ones. Thus it is possible to obtain information on its relative importance for the model (compared to that of B3, for instance).

On the (100) surface, the smallest cluster, $\text{Ni}_{17}(12,5)$, again consists of A1 and B1 and the nearest neighbors within the first and second layer, A2 and B2, respectively. The largest cluster, $\text{Ni}_{29}(16,9,4)$, is derived from Ni_{17} , extending it by three groups of four atoms, A3 in the first, B3 in the second, and C1 in the third crystal layer. To analyze the influence of each of the various groups of atoms separately, a comparison is carried out with alternative clusters of intermediate size, $\text{Ni}_{21}(16,5)$, $\text{Ni}_{21}(12,9)$, and $\text{Ni}_{21}(12,5,4)$ (see Table II).

$\text{Ni}_{12}(6,6)$ and $\text{Ni}_{13}(6,7)$ are the smallest models used for the fcc and hcp site on Ni(111), respectively. Each consists of two groups of atoms (A1, A2) in the first and two (B1, B2) in the second layer. Only the fcc models are shown in Fig. 1. Formally, the hcp clusters may be derived from the fcc models by exchanging and relabeling the atoms from the second and the third substrate layers ($B \leftrightarrow C$). The clusters are extended into the third layer by two groups of atoms, C1 and C2, resulting in models of 19 substrate atoms in each case. Parallel series of clusters, starting with $\text{Ni}_{18}(12,6)$ and $\text{Ni}_{19}(12,7)$, respectively, probe the importance of A3, a group

of six symmetry equivalent atoms in the first layer. They lead to the largest models of the (111) surface, $\text{Ni}_{25}(12,6,7)$ and $\text{Ni}_{25}(12,7,6)$.

One of the intermediate clusters representing the fcc site, $\text{Ni}_{18}(6,6,6)$, is peculiar, as here C2 is included, but not C1, leaving a central hole in the third layer. It was constructed under the assumption that the primary effect of adding substrate atoms in the third layer comes from a more realistic description of the environment of B1 and B2. In this sense, "more is better" and a larger effect can be expected from adding C2, a group of six atoms. To justify this procedure, $\text{Ni}_{19}(6,6,7)$ (which includes C1) is studied for comparison.

Each series of models is terminated by a cluster built of seven groups of symmetry equivalent substrate atoms. At this size a satisfactory degree of convergence is reached for many observables in favorable cases. Of course, it would be worthwhile to corroborate this conclusion by extending the substrate cluster even further. This would be especially desirable in those cases, where convergence is still poor at the present maximum cluster size. Taking into account the substantial demand of computational effort necessary for a further increase of the cluster model size, the justification for an all-electron calculation seems questionable. Also, technical problems encountered in the calculations (slow SCF convergence) may become overwhelmingly large. Therefore, considering the capability of the method used, the present limitation of cluster size appears to be an adequate compromise.

III. RESULTS AND DISCUSSION

A. Cluster convergence

With increasing size of the cluster models one expects a stabilization of the calculated quantities. In most cases this is fulfilled, indeed, to a satisfactory degree, i.e., with relative differences of a few percent between corresponding quantities of the two largest clusters of a series. In some cases, however, variations of more than 10% occur. This is demonstrated by the results compiled in Table III. Starting with some general observations, this section presents a discussion of the different cluster series under three main aspects. Of course, the principal issue is whether or not convergence in the calculated properties is found among the clusters chosen to model a particular situation. Closely connected to this is an analysis of the sensitivity of the various quantities with respect to cluster size. Finally, a detailed comparison will shed light on the construction of cluster models from a systematic viewpoint.

Table III gives the equilibrium position $d_{\perp}(\text{eq})$ of the adsorbate and the corresponding distance to the nearest first-layer substrate atom A1. Differences in the former appear somewhat attenuated (and thus concealed) in the latter due to their geometric relationship. The frequency ω_{\perp} is determined under the assumption of a rigid substrate, neglecting any coupling to the substrate phonons. This affects the comparison with experiment (see below), but it does not play a role for the evaluation of the convergence behavior. The binding energy is also given in Table III. These properties are supplemented by the induced dipole moment $\Delta\mu(d_{\perp})$, plotted in Figs. 2(a)–2(d) as a function of the adsorbate position.

TABLE III. Calculated values for the equilibrium distance $d_{\perp}(\text{eq})$, the nickel–sulfur distance $d(\text{NiS})$, the vibrational frequency ω_{\perp} , and the binding energy BE of Ni/S. The sulfur chemisorption at the nickel (100), (110), and (111) surfaces is modeled by the clusters introduced in Table II.

Surface	Ni_nS	$d_{\perp}(\text{eq})$ (Å)	$d(\text{NiS})^a$ (Å)	ω_{\perp} (cm^{-1})	BE (eV)
110	11	0.79	2.30	368	5.98
	13	0.84	2.31	321	5.81
	15	0.91	2.34	296	5.74
	17	0.93	2.35	286	5.66
	21	0.90	2.34	291	6.28
100	17	1.39	2.24	315	6.02
	21(16,5)	1.39	2.24	314	5.96
	21(12,9)	1.36	2.22	320	6.66
	21(12,5,4)	1.31	2.19	305	6.03
	29	1.30	2.19	309	6.48
111 ^b	12	1.56	2.12	381	5.82
	18(6,6,6)	1.55	2.12	353	5.40
	19	1.56	2.12	360	5.41
	18(12,6)	1.57	2.13	397	5.80
	25	1.59	2.14	366	5.19
111 ^c	13	1.58	2.14	365	5.67
	16	1.56	2.12	374	6.15
	19(6,7,6)	1.57	2.13	338	5.66
	19(12,7)	1.57	2.13	395	5.89
	22	1.55	2.12	387	5.67
	25	1.58	2.14	365	5.36

^aEquilibrium bond distance to A1.

^bfcc site.

^chcp site.

1. Ni(110)/S

The results for the largest cluster among the (110) models, Ni_{21} , may be considered well converged. Comparing them to those of Ni_{17} one finds only slightly different values for $d(\text{NiS})$ and ω_{\perp} and the induced dipole moment curves are in very good agreement too. An even smaller cluster, Ni_{15} , also gives quite similar values, but the resulting curve of the dipole moment displays a considerable positive shift at all distances [Fig. 2(a)]. On the other hand, the smallest models, Ni_{11} and Ni_{13} , both lead to a substantially larger frequency accompanied by a shorter equilibrium bond distance. In either case the dipole moment curve deviates substantially from the converged result.

Moving through the series one observes only small changes in $d(\text{NiS})$, yet large enough to appreciate a stabilization with growing cluster size. The influence of the model is reflected more vividly by the differences of ω_{\perp} . Its value drops by more than 70 cm^{-1} as the cluster grows from its minimal size of 11 atoms to a model differing by a group of 4 atoms only, Ni_{15} . But it then remains unchanged within 10 cm^{-1} , as more atoms are added to the cluster. The most dramatic sensitivity towards size and shape of the model is associated with the induced dipole moment $\Delta\mu(d_{\perp})$. While decreasing monotonically for the larger clusters, it exhibits a maximum for the smaller models. It is important to note that this qualitative difference could not have been foreseen if only the equilibrium values of $\Delta\mu$ (marked in Fig. 2) had been evaluated, since they lie rather close together.

Convergence of the binding energy is plagued by well-known problems.^{31,33} While this quantity seems to converge

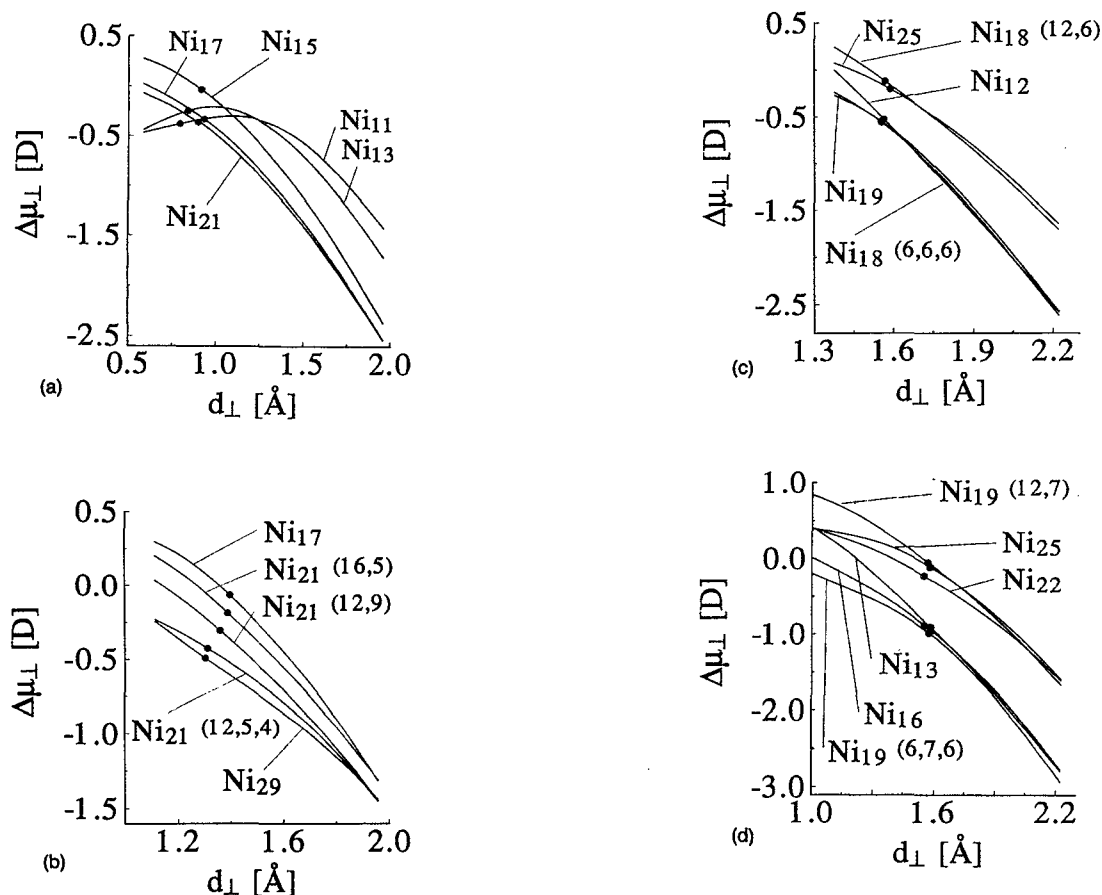
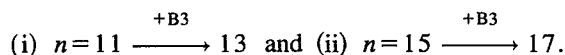


FIG. 2. The adsorbate induced dipole moment $\Delta\mu$ of Ni_nS as a function of the vertical adsorbate position d_\perp for cluster models of the surfaces (a) (110), (b) (100), (c) (111) fcc site, and (d) (111) hcp site. The equilibrium position is marked for each cluster.

(slowly) for the clusters Ni_n , $n=11, \dots, 17$, its trend is disrupted at $n=21$. Effects of the same order of magnitude have been reported [e.g., for $\text{Ni}(100)/\text{F}$] and explained³² from an analysis of the underlying bonding mechanism. Due to the use of the FON technique in the present approach, an analogous evaluation cannot be accomplished in a straightforward manner, but it is very likely that the origin of the effects is of similar nature.⁴⁵ For the same reason it is not possible to use the bond preparation concept as suggested by Siegbahn.³¹

Analyzing the convergence behavior described above we detect an obvious correlation to the structure of the cluster. Grouping the various models according to the presence or absence of the third substrate layer (Table II) reveals the relative importance of C1. The stabilizing effect of this group of atoms is demonstrated by a comparison of two pairs of cluster models Ni_n ,



The notation used here indicates that the clusters of each pair are related to one another by the introduction of the group B3 (see Table II), which results in a frequency change of almost 50 cm^{-1} in case (i), but only of 10 cm^{-1} for (ii). The same tendency, although weaker, is found for d_\perp (eq).

An alternative way of characterizing the substrate models is suggested in Table II. The coordination of the atoms A1

and B1 describes to which extent the true crystal environment of the adsorption site (see Table I) is represented in each cluster model. Only six nickel atoms adjacent to B1 (of a total of 11) are part of the smallest clusters, but B1 is almost saturated with its nearest neighbors in the larger models. This distinction may be correlated to the degree of convergence found for the different cases. Following this line of argument, the addition of the fourth layer atom D1 to the cluster should be considered. This would probably lead to an excellent candidate, if the cluster model were to be augmented further, since then the atoms which interact directly with the adsorbate (A1 and B1) would be completely surrounded by the nearest shell of substrate atoms.

2. $\text{Ni}(100)/\text{S}$

Striving for cluster convergence in the sense described above, the (100) surface presents an easy task. The construction of the largest cluster, Ni_{29} , which turns out to be quite a satisfactory model, is straightforward. Comparing it to the alternative clusters of intermediate size, $n=21$, one finds very close agreement in the case of $\text{Ni}_{21}(12,5,4)$ for the bond distance, the adsorbate vibrational frequency, and the dipole moment.

In the series Ni_n , $n=17 \rightarrow 21(12,5,4) \rightarrow 29$, the induced dipole moment again appears to be a sensitive measure of

cluster convergence which is also reflected by the equilibrium distance. On the other hand, the vibrational frequency does not vary much at all. Obviously it is already fairly well converged in the given range of cluster sizes, documenting to which precision this quantity can be extracted from cluster calculations in favorable cases. The convergence of the binding energy, although less awkward than for the Ni(110)/S cluster series, is not very satisfactory.

Taking into account the alternative clusters Ni₂₁(16,5) and Ni₂₁(12,9), the relative importance of an extension into the third layer (C1) over the addition of further atoms in the first (A3) or second (B3) layer may clearly be established from Table III and Fig. 2. For these model clusters, the calculated geometry and the induced dipole moment both deviate from the converged result to a larger degree than in the case of Ni₂₁(12,5,4). Alternatively, this observation can again be described in terms of the coordination of A1 and B1, the atoms forming the adsorption site. The former does not change much as the cluster size and shape is varied, but the latter grows by 50%, attaining its maximum value in Ni₂₁(12,5,4) and Ni₂₉ (see Tables I and II). This observation may be taken as a clue that an adequate description of B1 (i.e., a bulklike environment beneath the adsorption site) has considerable influence on the quality of a cluster model of the (100) fourfold hollow site.

3. Ni(111)/S

In both series of Ni(111) model clusters, the equilibrium bond distance $d_{\text{NiS}}(\text{eq})$ is quite independent of the cluster size. The opposite is true for the frequency of the vertical adsorbate vibration, ω_{\perp} , which changes substantially with each additional group of atoms, even at large cluster sizes. A more detailed analysis of this behavior, revealing some systematic aspects, is given below. Taking the induced dipole moment [Figs. 2(c) and 2(d)] as an indicator of convergence, one finds a clear separation of the models into two groups. Apart from this splitting, however, the differences in the curves are strikingly small at the equilibrium distance and beyond.

Two different aspects play a role in the construction of the clusters. The results discussed for the surfaces (100) and (110) suggest that the influence of a third crystal layer (C1 and C2) should be tested. On the other hand, we want to study the effect of extending the first layer (A3). Forming all possible combinations, one has the chance to trace the origin of some peculiarities of the (111) adsorption sites.

A pairwise comparison of clusters shows that the calculated frequency shifts are not at random, but follow certain trends. The effect of A3 on ω_{\perp} can be explored in five examples [Ni₁₂ vs Ni₁₈(12,6) and Ni₁₉ vs Ni₂₅ for the fcc site; Ni₁₃ vs Ni₁₉(12,7), Ni₁₆ vs Ni₂₂, and Ni₁₉(6,7,6) vs Ni₂₅ for the hcp site, see Table II]. An increase of 6–30 cm⁻¹ is found. The complementary analysis of four pairs of clusters [fcc: Ni₁₂ vs Ni₁₉ and Ni₁₈(12,6) vs Ni₂₅; hcp: Ni₁₃ vs Ni₁₉(6,7,6) and Ni₁₉(12,7) vs Ni₂₅] demonstrates that the additional substrate atoms (C1+C2) lower the vertical vibrational frequency of sulfur by 20–30 cm⁻¹. The presence or absence of A3 leads to a suitable classification of the cluster models, which is also quite helpful in the interpretation of

the dynamical dipole moment [Figs. 2(c) and 2(d)]. Here we find the influence of C1 and C2 to be comparatively small. These atoms lead to a splitting at very short adsorbate–substrate distances which almost disappears above the equilibrium distance. On the other hand, the presence of A3 is obviously correlated to a large separation of the dipole moment curves at all distances.

The considerable effect of A3 is not too surprising if one realizes that its geometric relationship to the adsorbate is similar to that of A2 in the case of the (100) and (110) adsorption site. In fact, due to the lower symmetry the largest (111) cluster Ni₂₅ has the same number of substrate atoms in the first crystal layer as Ni₁₇, the smallest model of the (100) surface. At the same time the influence of the third layer of atoms, though still conceivable, is smaller than for the other surfaces. The contributions of C1 and C2, respectively, are similar for the clusters modeling the hcp site. For the fcc models, an imbalance is observed. This is due to the fact that C2 represents a group of six atoms, whereas C1 is a single atom. Comparison of Ni₁₈(6,6,6) and Ni₁₉ clearly shows that C1 has little influence in this case; the small difference of the binding energies must be considered somewhat fortuitous for reasons discussed previously.

Summarizing, we find that in terms of convergence the (100) surface presents the least difficulties. It is harder to obtain converged results for Ni(110), but with some effort it can be achieved. Applying the same standards, both (111) cluster series must be considered as poorly converged. The representation of chemisorption sites by clusters of 20–30 substrate atoms can successfully be used to calculate adsorbate–substrate bond distances within 0.02 Å. For the vertical frequency, an uncertainty of 20 cm⁻¹ is exceeded only in unfavorable cases, but a convergence to about 5 cm⁻¹ may be reached. This is a clear improvement over the results found for smaller clusters.³³ There, bond length differences of 0.4 to 0.1 Å occur and frequencies vary by about 10 cm⁻¹, but these numbers may not be representative, as the study is by no means systematic or even complete regarding the selection of clusters.

An inspection of the curves in Fig. 2 shows that the adsorbate induced dipole moment is stabilized to approximately 0.1 D. For the binding energy, an estimate of the cluster error does not seem meaningful, since without special treatment (see above) convergence can hardly be found in the data presented here and would not be expected even at much larger cluster sizes.³⁶

B. Evaluation of the converged results

So far, only theoretical results have been compared to each other. Of course, an essential question is to which degree the converged results agree with information derived by various experimental techniques. To some extent, this problem has been tackled in a previous account.² There is a large body of experimental material available for the chemisorption system Ni/S which requires careful and critical interpretation.^{1–22} It is especially ample with respect to geometrical aspects, but also covers dynamic (ω_{\perp}) and energetic BE properties. During the following discussion, some systematic differences between the model and the experimental

situation should be kept in mind: (i) cluster models feature rigid (bulk) distances between the substrate atoms and do not take into account surface relaxation or reconstruction;⁴⁶ (ii) neglecting adsorbate–adsorbate interaction in the model prohibits the observation of any effects related to a variation of the coverage. This has consequences mainly for the comparison of geometry related results which will be discussed below (Sec. III B 1).

The evaluation of the converged results can be carried out under yet another aspect. Some quantities may be obtained from the theoretical treatment for which experimental information is scarce or not available at all. Interpretation of the charge distribution, the electronic structure, the magnetic properties, etc., may be conceptually helpful for understand-

ing the adsorbate–substrate interaction (Secs. III B 3 and III B 4).

Having settled the question of convergence in Sec. III A, we will subsequently use the results obtained from the largest clusters of each series. Therefore, in the current section (and in Tables IV and V) Ni(110)/S is represented by the cluster Ni₂₁S, Ni(100)/S by Ni₂₉S, and Ni(111)/S by Ni₂₅S (fcc), unless stated otherwise.

1. Equilibrium bond distances

All standard methods of surface structural analysis have been applied to the adsorption of sulfur at the three low index surfaces of nickel (see Table IV). Low-energy diffrac-

TABLE IV. Experimental and theoretical equilibrium distances (in Å) of various Ni/S systems. For geometric reasons, on different surfaces the distances denoted d_{NN} and d_{NNN} refer to different nickel atoms (see the footnotes to the calculated values).

System	Method	$d_{\perp}(\text{eq})$	$d_{NN}(\text{eq})$	$d_{NNN}(\text{eq})$	Δ^a	Reference
Ni(110)						
Cluster (calc.)	LDF	0.90	2.14 ^b	2.34 ^c		this work
$c(2 \times 2)$ (expt.)	LEED	0.93	2.17	2.35	± 0.1	4
		0.84	2.21	2.32	± 0.03	5
	ion scattering	0.87	2.18	2.32	± 0.03	10
		0.89	2.14		± 0.05	11
	SEXAFS		2.19	2.31	± 0.03	12
			2.23	2.31	± 0.04	13
	ARPEFS ^d	0.81	2.20	2.31	± 0.02	17
Ni(100)						
Cluster (calc.)	LDF	1.30	2.19 ^c	3.06 ^b		this work
	HF	1.28				23
	GVB	1.24				47
Slab (calc.)	LDF	1.36				24
$p(2 \times 2)$ (expt.)	LEED	1.30	2.19		± 0.1	6
		1.25	2.16	3.07	± 0.03	7
$c(2 \times 2)$ (expt.)	LEED	1.30	2.18	3.06	± 0.1	4
		1.30	2.19	3.10	± 0.08	8
	ion scattering	1.40	2.25		± 0.05	11
			2.23		± 0.02	14
	SEXAFS		2.24			18
			2.19		± 0.03	19
	NPD ^e	1.31			± 0.04	20
	EELS	1.30				21
		1.35				
Ni(111)						
Cluster (calc.)	LDF	1.59	2.14 ^c	3.28 ^f		this work
$p(2 \times 2)$ (expt.)	LEED	1.40	2.02	2.93	± 0.1	4
		1.50	2.10		± 0.02	9
	ion scattering	1.61	2.16		± 0.06	11
			2.20		± 0.04	12
	SEXAFS		2.23	3.35	± 0.03	15
		1.69				22
	INS ^g	1.78				22
$5) \times 2$ (expt.)	SEXAFS		2.18		± 0.04	12
			2.27		± 0.02	15
			2.22		± 0.03	16

^aMax. experimental error estimate.

^bDistance to B1.

^cDistance to A1.

^dAngle-resolved photoelectron fine structure.

^eNormal photoelectron diffraction.

^fDistance to A2.

^gIon neutralization spectroscopy

TABLE V. Nominal charge difference and change in magnetization induced by sulfur chemisorption. The quantities, calculated from Mulliken population analysis of the clusters Ni_{21}S for Ni(110), Ni_{29}S for Ni(100), and Ni_{25}S for Ni(111) (fcc site), are given per atom for each group of symmetry-related atoms and as the sum taken over the whole substrate cluster.

Group of atoms	Chemisorption induced change of					
	Nominal charge			Spin polarization		
	Ni(110)	Ni(100)	Ni(111)	Ni(110)	Ni(100)	Ni(111)
A1	0.10	0.12	0.03	-0.24	-0.38	-0.24
A2	0.01	0.00	0.08	-0.01	-0.02	-0.05
A3		0.01	0.00		0.00	-0.02
B1	-0.08	0.10	-0.01	-0.15	0.01	0.00
B2	0.07	-0.04	0.01	0.00	-0.02	-0.04
B3	-0.01	0.00		0.04	-0.12	
B4	-0.00			-0.08		
C1	-0.02	0.00	0.00	0.02	-0.03	0.00
C2			0.00			0.03
Σ^a	0.48	0.47	0.31	-1.33	-2.30	-0.97

^aSum over all nickel atoms.

tion (LEED),⁴⁻⁹ ion scattering,^{10,11} and surface enhanced x-ray absorption fine structure (SEXAFS)¹²⁻¹⁶ measurements exist for all of them. On each surface additional investigations have been carried out using a variety of other methods¹⁷⁻²² that also yield information about the adsorption geometry. For reason (i) given above, a comparison to experiment should not be restricted to a single bond distance. Indeed, most experimental accounts provide $d_{\perp}(\text{eq})$, the vertical spacing between the adsorbate and the first substrate layer as well as the sulfur-nickel bond distances to the nearest and next-nearest neighbors, $d_{\text{NN}}(\text{eq})$ and $d_{\text{NNN}}(\text{eq})$. Clearly, in our models two of them are redundant, but assuming that the equilibrium condition is a function of the interaction between sulfur and the various substrate atoms, it is meaningful to compare all three of them to the corresponding experimental distances.

As already mentioned, the validity of the comparison also depends on the degree to which adsorbate-adsorbate interactions play a role in a given experimental situation. Data for different coverages (where available) have been included in Table IV. An estimate of the effect due to additional adatoms has been attempted previously, based upon an extended model Ni_{21}S_5 of the (110) surface.² The Ni_{21} cluster permits only a rather approximate study of the sulfur coverage corresponding to the $c(2 \times 2)$ overlayer found experimentally, since the adatoms at the fringe of the cluster (located above B4) lack most of their substrate neighbors. Indeed, the imbalance of the adsorbate-to-substrate ratio should lead to an overestimation of the corresponding effect. The change of $d_{\perp}(\text{eq})$ observed, however, amounted to only 0.01 Å, the frequency shifted by less than 10 cm^{-1} .² This is coherent with the results obtained by Bauschlicher and Bagus²³ for the analogous investigation of sulfur on Ni(100), ascertaining that an increase of the sulfur coverage has little effect on both the bond length and the vibrational frequency.

On Ni(110), a $c(2 \times 2)$ structure is formed at $\theta=0.5$ ML. The differences between the results obtained from different measurements (and different methods) are acceptable, but in some cases larger than the estimated experimental errors

would suggest. The theoretical results lie well within the range of the experimental values. In the calculation, there seems to be a tendency to overestimate $d_{\perp}(\text{eq})$, but to underestimate $d_{\text{NN}}(\text{eq})$, which is the bond distance to the second layer nickel atom beneath the adsorbate (B1). This may be interpreted to reflect the lack of flexibility of the cluster, resulting in a structural compromise. Experimentally, the interlayer distance between the first and second layer is found to exceed the bulk value by 10% upon sulfur adsorption.⁵ This structural change may be compared to the contraction of the layer distance in the bare surface by about 8% with respect to the bulk.⁵ A reproduction of this chemisorption induced change is beyond the capabilities of the present cluster models.

On the (100) surface, a sulfur coverage of $\theta=0.25$ ML, corresponding to a $p(2 \times 2)$ structure can be observed. Comparison to the $c(2 \times 2)$ structure shows that an increase in coverage (to $\theta=0.5$ ML) has little effect on the bond distances (see Table IV). From our theoretical treatment we obtain results that are in good agreement with experiment. It must be taken into account, however, that it is not possible to fully satisfy all experimental data given in Table IV simultaneously. Earlier cluster calculations,^{23,47} yielding a somewhat smaller vertical adsorbate-substrate distance than our model, are still within the range of experimental errors. A larger distance found in a $c(2 \times 2)$ slab calculation²⁴ lies also in this range (see Table IV).

The $p(2 \times 2)$ structure observed on the Ni(111) surface at low coverage ($\theta=0.25$ ML) is characterized somewhat differently by different experimental methods. For example, taking the most recent LEED experiment⁹ as a reference, the theoretical values appear to be too large. On the other hand, when compared to recent SEXAFS results,¹⁵ the calculated equilibrium distances are found to underestimate the experimental value considerably. The calculated result does, however, agree very well with ion scattering data.¹¹ This comparison once more highlights the difficulties encountered in the analysis of the chemisorption system Ni(111)/S.

2. Adsorbate vibration and binding energy

A detailed comparison between the calculated vibrational frequencies and the data from electron energy loss spectroscopy (EELS) has been given elsewhere.² Experimental results are available for sulfur chemisorbed at Ni(110) and Ni(100). The frequencies lie at higher values than the theoretical ones. To some degree this is due to the fact that in the model neither a lateral displacement of the adsorbate nor substrate vibrations are taken into account. Freezing these degrees of freedom leads to uncoupled mode frequencies of $\omega_{\perp} = 291$ and 309 cm^{-1} , respectively, about 40 cm^{-1} below the experimental frequencies which are observed for a $c(2 \times 2)$ overlayer, 331 cm^{-1} at Ni(110)² and 351 cm^{-1} at Ni(100).³ An even larger frequency, 367 cm^{-1} , has been reported at a lower coverage for Ni(100)/ $p(2 \times 2)\text{S}$.³ It has been pointed out that the effect of coverage is only marginal for sulfur adsorption in sharp contrast to oxygen adsorption.²³ Indeed, the coverage dependence is rather small compared to the systematic deviation discussed above. Apart from these aspects, however, the calculated frequencies properly reproduce the experimental trend, i.e., they increase with decreasing coordination of the adsorbate (see Table I).

The calculation of chemisorption energies presents a twofold problem. Besides the question of cluster convergence which has already been addressed (Sec. III A), one observes overbinding. This is found for Ni(100) (expt. BE = 4.26 eV) as well as for Ni(111) (expt. BE = 4.40 eV).¹ For this reason, the theoretical binding energy values of the present study must be considered to be of limited value only.

3. Adsorbate charge, population changes, and spin quenching

In Sec. III A the induced dipole moment has been used to characterize the convergence with cluster size for each cluster series. Under the assumption that its variation with geometry is caused by the movement of the partially charged adsorbate only, its slope can be viewed as an effective charge.^{41,48} This interpretation, however, neglects polarization effects within the substrate cluster and requires the variation of the dipole moment to be linear⁴⁸ which is obviously not the case (Fig. 2). As the chemical interaction between the adsorbate and the substrate decreases (i.e., with increasing separation) the curvature of the dipole moment curve is expected to become smaller. This is indeed found at a height of $d_{\perp} \approx 2 \text{ \AA}$. In this region the corresponding effective charge of sulfur has a value of -0.6 to $-0.4 e$ as compared to ≈ -0.3 to $-0.2 e$ at equilibrium distance. Clearly, the electronegative adsorbate picks up some charge, as one would expect, but it is hardly possible to determine the exact amount at equilibrium in this way.

The result is in general accordance with evidence from a Mulliken population analysis which assigns a charge of -0.3 to $-0.5 e$ (depending on the surface) to the adsorbate at equilibrium. These values, too, vary with d_{\perp} (differences of 0.2 to $0.3 e$ occur), an effect which is partially due to the fact that diffuse basis functions localized on sulfur penetrate the region of high (nickel d band) electron density as the adsorbate approaches the surface.

A somewhat smaller ionicity of sulfur is determined from the high coverage model for the (110) surface mentioned previously.² There, as in the cases discussed above, the predicted adsorbate charge exceeds the effective charge determined from experimental vibrational intensity. Further studies are necessary to investigate this discrepancy.

The population analysis, although only of limited value for the reasons given above, serves as a valuable tool to trace the net charge flow within the cluster. The differences in population caused by the adsorbate-substrate interaction are more reliable than their absolute values and they can be used to describe the redistribution of electronic charge upon chemisorption. This can be done separately for both orientations of the electronic spin. Thus it is possible to analyze spin quenching effects on each group of nickel atoms (Table V).

In the following discussion, two important aspects are addressed, one of methodological and one of physical nature. As the cluster approach operates under the assumption of localized interactions, a violation of this presupposition must be assumed if the edge atoms of the finite surface segment represented by the cluster display changes of comparable magnitude as those in the immediate vicinity of the adsorbate. Furthermore, for the understanding of sulfur as a catalytic poisoner it is important to explore how many metal atoms are affected by the adatom.^{24,25,28,49-52} This question eventually requires a more detailed study of the local electronic structure (see Sec. III B 4).

Electronic charge is transferred to the adsorbate, leaving behind a positively charged substrate cluster (Table V). On Ni(100) this charge is clearly localized at A1 and B1. Considering the slightly negative charge at B2 (a group of four atoms), one finds almost no net charge transfer beyond the first layer. Indeed, the electronic rearrangement within the second layer (involving an edge atom!) would probably be attenuated even more if more atoms were added to the cluster. This tendency is deduced from a comparison of Ni₁₇ and Ni₂₁(12,9) which differ by the presence of the atoms B3. A similar situation is found on Ni(110) where essentially only the groups A1, B1, and B2 are affected. Again, the changes in nominal charge can be interpreted as an intralayer polarization in the second crystal layer and a depletion of electronic density at A1.

Adsorption at the threefold sites of the (111) surface shows several peculiarities. In the top layer, the atoms A1 and A2 supply electronic charge to the adsorbate, more than half of it coming from A2. This ratio is somewhat smaller for the alternative Ni₂₅ cluster representing the hcp site; there the chemisorption induced charge difference at A1 and A2 is 0.05 and 0.07 per atom, respectively. The observation that A2 is strongly involved provides additional evidence for the fact that the atom group A3 plays an important role for the present cluster (cf. Sec. III A 3). Indeed, one might want to extend the first layer even further. There is almost no change of population in the second and third layer.

The quenching of magnetic moments by the adsorbate, i.e., the decrease of spin polarization, is another useful means of characterizing the range of interaction. A local reduction of substrate magnetism, e.g., well known from the study of CO on nickel,⁵³⁻⁵⁵ can be expected to take place in the sys-

tem Ni/S too. A recent investigation of the spin quenching in large cluster carbonyl compounds has shown³⁸ that a considerable magnetic moment survives even at metal atoms that are next-nearest neighbors to the ligands, demonstrating that the quenching of spin density is a rather localized effect.

The magnetization of 0.6 to 1.0 μ_B per atom found in the bare cluster is reduced in most cases upon chemisorption (Table V). As one would expect from results of recent cluster studies modeling atomic (H,C,O) and molecular (CO) adsorption on Ni(100),^{56,57} the nearest neighbors in the first layer are affected most strongly. Of course, on the (110) surface with its open structure, the magnetism of B1 is attenuated too. But beyond this it is interesting to find a non-negligible decrease of spin density in the second layer. It is largest for the atoms B3 of Ni(100), but also observable for B4 of Ni(110) and B2 of Ni(111), displaying a trend which parallels that in the values for A1. It is worth mentioning that each of the affected atoms lies approximately in one line with the substrate atom A1 and with the adsorbate atom. Apparently, sulfur reduces the spin polarization of A1 which in turn affects the spin polarization of the next atom in the same direction.

Except for this effect the edge atoms of the clusters are not subject to noticeable changes in their magnetization. This leads to the conclusion that in all cases considered an adequate description of spin quenching effects is not limited by the current cluster size. Indeed, some of the peculiarities of the induced charge difference (conjectured to be cluster artifacts above) do not appear in the analysis of spin differences. Summarizing one may state that for the clusters used in the present study the net redistribution of charge and the reduction of spin polarization is fairly localized, justifying the cluster approach.

4. Local density of states

The reduced catalytic activity of poisoned metal surfaces is due to a site blocking effect and may also involve electronic effects. In the case of electronegative adatoms (e.g., sulfur), kinetic investigations clearly indicate a mechanism that goes beyond simple site blocking.²⁹ The range to which surface atoms are affected by the modifier atom has been discussed controversially.^{24,25,28,49–52} Experimental studies using coadsorbed CO molecules as a probe have been interpreted to contradict a long-range electronic effect.^{49,50} Several theoretical investigations have been undertaken for such systems. Among them, slab calculations of Rh(100)/X (X=P,S,Cl,Li)⁵¹ and cluster model studies of M(111)/S (M=Ni, Rh)²⁵ have been analyzed for electronic effects which might play a role in a mechanistic model of poisoning. The conclusions drawn are in favor of mechanisms that include long-range electronic effects. It seems worthwhile to evaluate quantities similar to those upon which their arguments are based.

MacLaren *et al.* (Ref. 25, and references therein) suggest to use the local density of states (LDOS) and its changes upon chemisorption as an indicator of poisoning. Treating sulfur adsorption on Ni(111), they consider situations that are complementary to our construction in the sense that the reference point (i.e., the point where the DOS is evaluated) lies

on the z axis and is surrounded by 3, 6, or 12 adsorbate atoms at the near, far, or remote adsorption site, respectively. Despite the different approach, the mutual geometric relationship between sulfur and the reference point can simply be transferred to the Ni₂₅S cluster model by projecting the DOS to the atom groups A1, A2, and A3, respectively. In the total DOS [Fig. 3(a)] the adsorbate causes only small differences: it is the average over seven different groups of substrate atoms. Even for the bare cluster the contributions of these groups vary noticeably [solid lines in Figs. 3(b)–3(d)], but the gross features of the Ni d manifold are well reproduced in each case. Considering A1 (in relation to which sulfur occupies the “near site”²⁵), the DOS changes dramatically. At the Fermi level E_F , the minority spin DOS is reduced by 50%, whereas the majority spin DOS increases which results in the quenching of the magnetic moment discussed above (cf. Table V). Changes are visible over the whole d manifold DOS [only d contributions have been included in Figs. 3(b)–3(d)]. Sulfur at the “far site” (DOS at A2) causes a slight increase of the DOS at E_F and a moderate deformation of the d band [Fig. 3(c)]. In the projection to A3 (corresponding to sulfur at the “remote site”) only minimal changes appear in the DOS curve [Fig. 3(d)]. These observations qualitatively resemble the results reported by MacLaren *et al.*²⁵ although we consider the influence of a single modifier atom only.

The above analysis is based on Mulliken populations and therefore suffers from the deficiencies mentioned before. Furthermore, the distribution of electronic charge in space is described only in a rather crude way (i.e., per atom). A more detailed picture requires the spatial resolution of the charge density before and after chemisorption. At the same time, however, we would like to preserve the energetic resolution because it carries information of physical relevance as the changes in the DOS are energetically not uniform [Figs. 3(b)–3(d)]. A comparison may be achieved by evaluating the electronic density in an energy window defined by a Gaussian weighting of 0.5 eV width centered at a given energy (in analogy to a suggestion by Feibelman and Hamann⁵¹). As an example, the density difference between Ni₂₅S and Ni₂₅ is shown (Fig. 4) for different energies and different planes through the cluster. The first plane contains all surface centers (A1, A2, and A3). The second plane is defined by a row of four atoms of the first layer (A3–A1–A1–A3) and three atoms of the second plane (B2–B1–B2); it does not pass through the position of the sulfur atom although the distance is small (0.36 Å). Only the minority spin density levels are used in Fig. 3; for the majority spin the results are similar, but shifted to lower energies by about 1 eV.

Considering the characteristic features of the DOS plots in Fig. 3, it is not surprising to find a depletion of electronic density at A1 and an increase at A2 and A3 at the Fermi energy [Fig. 4(a)]. Figure 4(b) shows that the decrease of the minority spin density also affects the B2 atoms in the second layer. In fact, these are the atoms for which a considerable quenching of the magnetic moment is observed (see Table V).

Based on this evidence the effect of the electronegative adsorbate might be classified as localized. In the case of

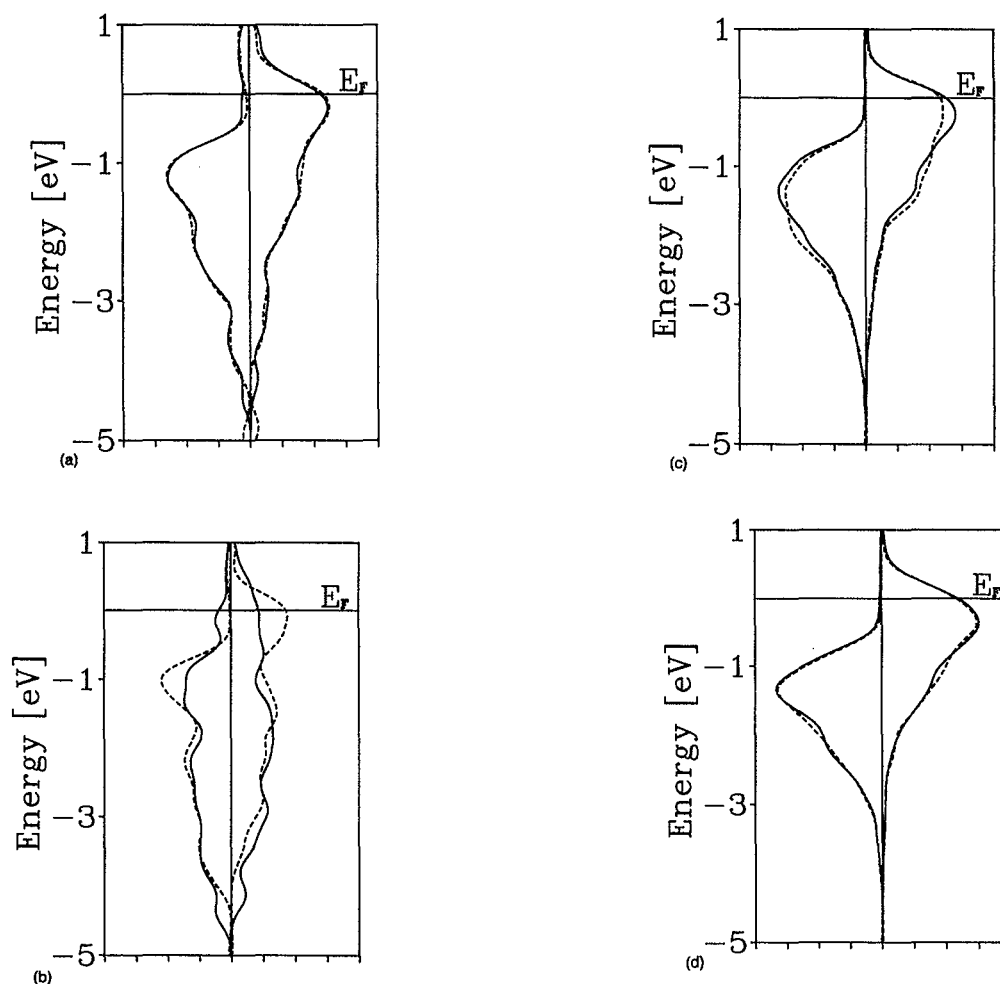


FIG. 3. Density of states (DOS) of the Ni(111) cluster models Ni_{25}S (solid) and the Ni_{25} (dashed) projected onto groups of nickel atoms: (a) total DOS; (b) DOS at A1; (c) DOS at A2; (d) DOS at A3. The curves (b)–(d) contain only Ni-*d* contributions and have been scaled by $25/n$, where n is the number of atoms of a group considered (A1, A2: $n=3$; A3: $n=6$).

Rh(100)/S a depletion of the DOS at the Fermi energy was found to extend beyond the nearest-neighbor atom of the first substrate layer.⁵¹ On Ni the opposite seems to be the case: the DOS increases at A2 and A3. On the other hand, Figs. 3(c) and 3(d) show that a reduction in the DOS for A2 and A3 does take place at 1 eV below the Fermi energy. These long-range electronic effects are observable very clearly in Figs. 4(c) and 4(d). They are, however, restricted to this energy window, since similar evaluations at various other energies display a rather localized redistribution of charge.

This comparison shows that the poisoning effect by an adsorbate may be connected to changes in the electronic structure that are rather localized in energy. Of course, this will depend on the details of the interaction between the metal surface and the molecules involved in a catalyzed surface reaction. As a conclusion of the present study we find that sulfur adsorption leads to a characteristic decrease of the DOS at 1 eV below the Fermi energy which affects all surface atoms of the largest clusters used. This long-range modification of the electronic structure may well have an effect on other metal–adsorbate interactions taking place at remote sites.

IV. CONCLUSIONS

We have presented an extensive cluster model study of sulfur chemisorbed at various nickel surfaces. In the course of the investigation, we have focused on two important issues: the aspect of convergence with increasing cluster size and the physical relevance of the converged results.

Clusters of 20–30 substrate atoms proved to be well suited for a theoretical description of atomic chemisorption. The remaining uncertainty in bond distances was estimated to be about 0.02 Å, vibrational frequencies are stable to about 20 cm^{-1} . Satisfactory convergence of the binding energy cannot be achieved without utilizing more elaborate concepts.^{32,36} Beside these quantities, the induced dipole moment was used as a very sensitive probe of cluster convergence.

Comparing clusters of different size and shape, the importance of third layer atoms for an accurate modeling of chemisorption systems has been established. These atoms are essential for a representation of the (110) surface, but also play a role for the (100) and (111) surfaces. As the surface becomes more compact, an appropriate description appears

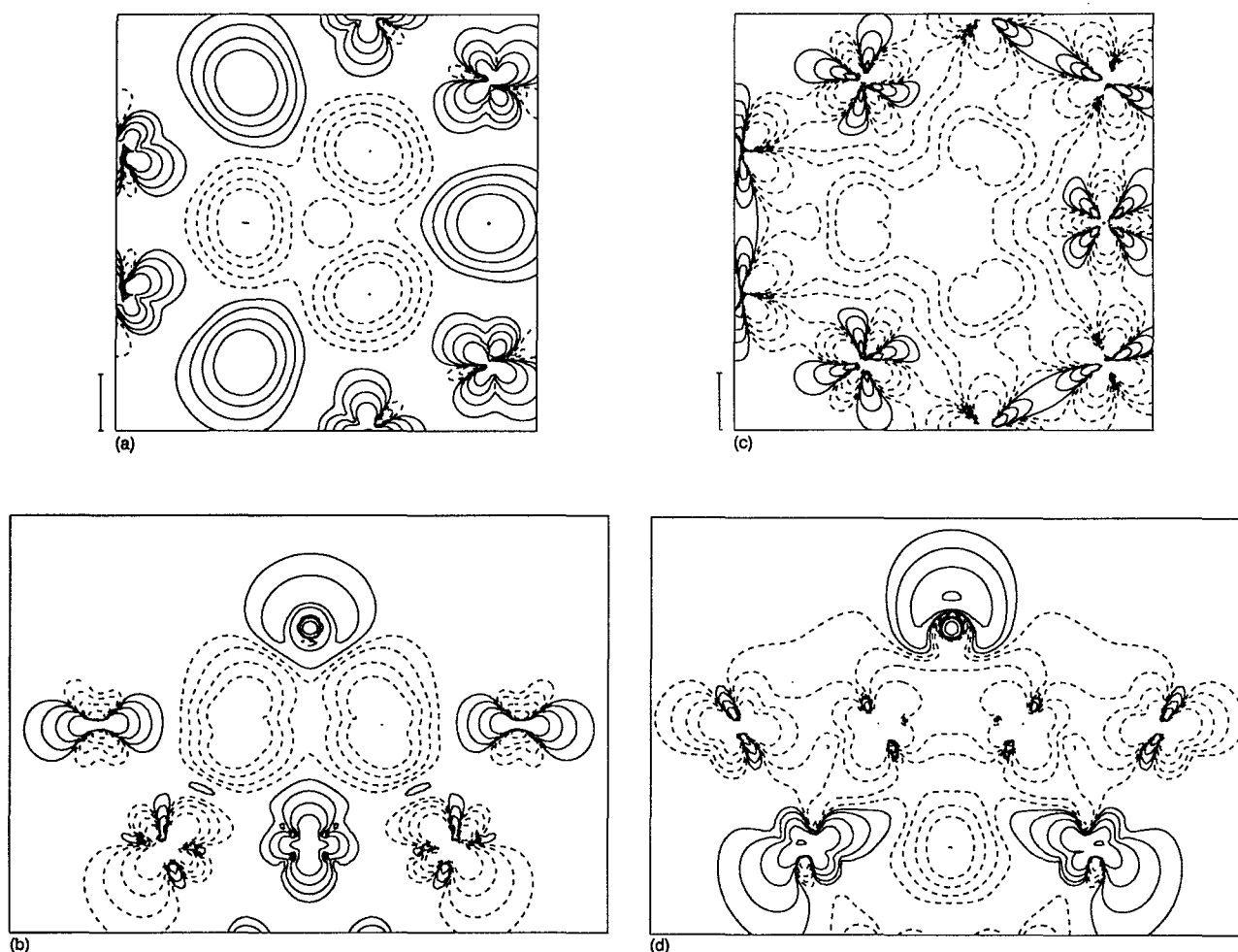


FIG. 4. Density difference (minority spin) of the (111) cluster models Ni_{25}S and Ni_{25} in different energy windows (see the text): at E_F (a and b) and at 1.0 eV below E_F (c and d). The first plane (a,c) passes through the centers of the first crystal plane (A1–A3). The other plane (b,d) passes through four substrate atoms in the first (A3–A1–A1–A3) and three substrate atoms in the second crystal plane (B2–B1–B2). The solid contour lines indicate positive, dashed lines negative density differences; their values are $10^{-3.5}$, $10^{-3.0}$, $10^{-2.5}$, and $10^{-2.0}$ a.u.

to require a third group of surface atoms (A3).

To check the quality and physical content of our approach, a comparison to experimental data has been presented. Adsorption induced electronic effects have been analyzed in light of other theoretical and experimental investigations.

Experimental bond distances are reproduced very well by our calculations. Due to the neglect of phonon coupling, the vibrational frequencies are determined too low by about 40 cm^{-1} .

Population analysis and dynamical dipole moment curves indicate that sulfur is partially negatively charged ($q \approx -0.3 e$). The nearest neighbors in the first substrate layer carry a positive charge which is screened very well, i.e., only minor charge rearrangements are induced on nickel atoms that are located farther away.

Local DOS curves also demonstrate the rather localized character of the adsorbate–substrate interaction. Charge density difference plots, however, reveal a long-range effect at about 1 eV below the Fermi energy.

ACKNOWLEDGMENTS

We thank G. Pacchioni for useful discussions as well as O. D. Häberlen and S. Krüger for their assistance during some of the calculations. This work has been supported by the Deutsche Forschungsgemeinschaft via SFB 338 and by the Fonds der Chemischen Industrie. We acknowledge a substantial grant of computer time from the Leibniz-Rechenzentrum München under the collaboration with Cray Research Inc.

¹ M. P. Kiskinova, *Surf. Sci. Rep.* **8**, 359 (1988).

² M. A. Chesters, D. Lennon, L. Ackermann, O. Häberlen, S. Krüger, and N. Rösch, *Surf. Sci.* **291**, 177 (1993).

³ S. Andersson, P. A. Karlsson, and M. Persson, *Phys. Rev. Lett.* **51**, 2378 (1983).

⁴ J. E. Demuth, D. W. Jepsen, and P. M. Marcus, *Phys. Rev. Lett.* **32**, 1182 (1974).

⁵ R. Baudouin, Y. Gauthier, and Y. Joly, *J. Phys. C* **18**, 4061 (1985).

⁶ M. Van Hove and S. Y. Tong, *J. Vac. Sci. Technol.* **12**, 230 (1975).

⁷ W. Oed, U. Starke, F. Bothe, and K. Heinz, *Surf. Sci.* **234**, 72 (1990).

⁸ U. Starke, F. Bothe, W. Oed, and K. Heinz, *Surf. Sci.* **232**, 56 (1990).

- ⁹Y. K. Wu and K. A. R. Mitchell, *Can. J. Chem.* **67**, 1975 (1989).
- ¹⁰J. F. van der Veen, R. M. Tromp, R. G. Smeenk, and F. W. Saris, *Surf. Sci.* **82**, 468 (1979).
- ¹¹Th. Fauster, H. Dürr, and D. Hartwig, *Surf. Sci.* **178**, 657 (1986).
- ¹²T. Ohta, Y. Kitajima, P. M. Stefan, M. L. Shek Stefan, N. Kosugi, and H. Kuroda, *J. Phys. (Paris)* **47**, C8, 503 (1986).
- ¹³D. R. Warburton, G. Thornton, D. Norman, C. H. Richardson, R. McGrath, and F. Sette, *Surf. Sci.* **189/190**, 495 (1987).
- ¹⁴S. Brennan, J. Stöhr, and R. Jaeger, *Phys. Rev. B* **24**, 4871 (1981).
- ¹⁵D. R. Warburton, P. L. Wincott, G. Thornton, F. M. Quinn, and D. Norman, *Surf. Sci.* **211/212**, 71 (1989).
- ¹⁶Y. Kitajima, T. Yokoyama, T. Ohta, M. Funabashi, N. Kosugi, and H. Kuroda, *Surf. Sci.* **214**, L261 (1989).
- ¹⁷S. W. Robey, J. J. Barton, C. C. Bahr, G. Liu, and D. A. Shirley, *Phys. Rev. B* **35**, 1108 (1987).
- ¹⁸J. J. Barton, C. C. Bahr, Z. Hussain, S. W. Robey, J. G. Tobin, L. E. Klebanoff, and D. A. Shirley, *Phys. Rev. Lett.* **51**, 272 (1983).
- ¹⁹J. J. Barton, C. C. Bahr, Z. Hussain, E. Umbach, and D. A. Shirley, *Phys. Rev. B* **34**, 3807 (1986).
- ²⁰D. H. Rosenblatt, J. G. Tobin, M. G. Mason, R. F. Davis, S. D. Kevan, D. A. Shirley, C. H. Li, and S. Y. Tong, *Phys. Rev. B* **23**, 3828 (1981).
- ²¹Z. Q. Wu, Y. Chen, M. L. Xu, S. Y. Tong, S. Lehwald, M. Rocca, and H. Ibach, *Phys. Rev. B* **39**, 3116 (1989).
- ²²G. E. Becker and H. D. Hagstrum, *Surf. Sci.* **30**, 505 (1972).
- ²³C. W. Bauschlicher, Jr. and P. Bagus, *Phys. Rev. Lett.* **54**, 349 (1985).
- ²⁴C. L. Fu and A. J. Freeman, *Phys. Rev. B* **40**, 5359 (1989).
- ²⁵J. M. Maclaren, J. B. Pendry, and R. W. Joyner, *Surf. Sci.* **178**, 856 (1986).
- ²⁶J. M. Maclaren, J. B. Pendry, D. D. Vvedendky, and R. W. Joyner, *Surf. Sci.* **162**, 322 (1985).
- ²⁷E. Wimmer, C. L. Fu, and A. J. Freeman, *Phys. Rev. Lett.* **55**, 2618 (1985).
- ²⁸M. C. Zonneville and R. Hoffmann, *Langmuir* **3**, 452 (1987).
- ²⁹J. A. Rodriguez and D. W. Goodman, *Surf. Sci. Rep.* **14**, 1 (1991).
- ³⁰*Cluster Models for Surface and Bulk Phenomena*, edited by G. Pacchioni, P. S. Bagus, and F. Parmigiani, NATO ASI Ser. B (Plenum, New York, 1992), Vol. 283.
- ³¹P. E. M. Siegbahn and U. Wahlgren, *Int. J. Quantum Chem.* **42**, 1149 (1992).
- ³²P. E. M. Siegbahn, M. A. Nygren, and U. Wahlgren, in *Cluster Models for Surface and Bulk Phenomena*, edited by G. Pacchioni, P. S. Bagus, and F. Parmigiani, NATO ASI Ser. B (Plenum, New York, 1992), Vol. 283, p. 267.
- ³³D. Post and E. J. Baerends, *J. Chem. Phys.* **78**, 5663 (1983).
- ³⁴I. Panas, J. Schüle, P. Siegbahn, and U. Wahlgren, *Chem. Phys. Lett.* **149**, 265 (1988).
- ³⁵N. Rösch and G. Pacchioni, in *Clusters and Colloids. From Theory to Applications*, edited by G. Schmid (Verlag Chemie, Weinheim, 1993).
- ³⁶L. G. M. Pettersson and T. Faxen, *Theor. Chim. Acta* **85**, 345 (1993).
- ³⁷B. I. Dunlap and N. Rösch, *Adv. Quantum Chem.* **21**, 317 (1990).
- ³⁸N. Rösch, L. Ackermann, and G. Pacchioni, *J. Am. Chem. Soc.* **114**, 3549 (1992).
- ³⁹R. G. Parr and W. Yang, *Density Functional Theory of Atoms and Molecules* (Oxford University, New York, 1989).
- ⁴⁰B. I. Dunlap, J. W. D. Conolly, and J. R. Sabin, *J. Chem. Phys.* **71**, 3396 (1979).
- ⁴¹N. Rösch, in *Cluster Models for Surface and Bulk Phenomena*, edited by G. Pacchioni, P. S. Bagus, and F. Parmigiani, NATO ASI Ser. B (Plenum, New York, 1992), Vol. 283, p. 251.
- ⁴²N. Rösch, P. Knappe, P. Sandl, A. Görling, and B. I. Dunlap, in *The Challenge of d and f Electrons. Theory and Computation*, edited by D. R. Salahub and M. C. Zerner, ACS Symp. Ser. No. 394 (American Chemical Society, Washington, D.C., 1989), p. 180.
- ⁴³A. Veillard, *Theor. Chim. Acta* **12**, 405 (1968).
- ⁴⁴S. H. Vosko, L. Wilk, and M. Nusair, *Can. J. Phys.* **58**, 1200 (1980).
- ⁴⁵P. Mlynarski and D. R. Salahub, *J. Chem. Phys.* **95**, 6050 (1991).
- ⁴⁶G. A. Somorjai and M. A. van Hove, *Progr. Surf. Sci.* **30**, 201 (1988).
- ⁴⁷T. H. Upton and W. A. Goddard III, *Phys. Rev. Lett.* **46**, 1635 (1981).
- ⁴⁸P. S. Bagus and G. Pacchioni, in *Cluster Models for Surface and Bulk Phenomena*, edited by G. Pacchioni, P. S. Bagus, and F. Parmigiani, NATO ASI Ser. B (Plenum, New York, 1992), Vol. 283, p. 233.
- ⁴⁹R. J. Madix, M. Thornburg, and S. B. Lee, *Surf. Sci.* **133**, L447 (1983).
- ⁵⁰M. Trenary, K. J. Uram, and J. T. Yates, Jr., *Surf. Sci.* **157**, 512 (1985).
- ⁵¹P. J. Feibelman and D. R. Hamann, *Surf. Sci.* **149**, 48 (1985).
- ⁵²S. R. Chubb and W. E. Pickett, *Phys. Rev. B* **38**, 10 227 (1988).
- ⁵³F. Raatz and D. R. Salahub, *Surf. Sci.* **146**, L609 (1984).
- ⁵⁴F. Raatz and D. R. Salahub, *Surf. Sci.* **176**, 219 (1986).
- ⁵⁵C. W. Bauschlicher, Jr. and C. J. Nelin, *Chem. Phys.* **108**, 275 (1986).
- ⁵⁶R. Fournier and D. R. Salahub, *Surf. Sci.* **238**, 330 (1990).
- ⁵⁷R. Fournier, J. Andzelm, A. Goursot, N. Russo, and D. R. Salahub, *J. Chem. Phys.* **93**, 2919 (1990).